Australian Journal of Crop Science

AJCS

AJCS 16(07):916-921 (2022) ISSN:1835-2707
doi: 10.21475/ajcs.22.16.07.p3568

Comparison between Matheron and Genton semivariance function estimators in spatial modeling of soybean yield

Gustavo Henrique Dalposso[1*], Miguel Angel Uribe-Opazo[2], Marcio Paulo de Oliveira[1]

[1]Federal University of Technology – Paraná (UTFPR), Toledo, Paraná, Brazil
[2]Western Paraná State University – (UNIOESTE), Cascavel, Paraná, Brazil

[*]Corresponding author: gustavodalposso@utfpr.edu.br

Abstract

In precision agriculture, interpolations are performed to map soybean yield, which facilitates decision making. Among the existing methods, geostatistics prevails, which uses information from the data's spatial structure to generate interpolated maps. The spatial dependence structure is modeled based on the semivariogram, with the Matheron semivariance estimator being the most commonly used function. However, studies show unreliability in the presence of outliers; therefore, other researchers propose an alternative use of the Genton semivariance function estimator. Despite several studies comprising comparative works involving both estimators of the semivariance function, there are only a few comparative studies considering theoretical semivariograms with cyclical behavior, such as the Wave model. This study, therefore, aims to compare these two estimators considering adjustments of the Wave model in soybean yield data, when containing an outlier. The spatial dependence measure index was used to measure the degree of the model's spatial dependence and the weighted Kappa index to assess the similarity of maps generated through kriging. It was possible to verify that the outlier removal was more impactful in the modeling considering the Matheron semivariance function estimator, thus confirming the robustness of the Genton semivariance function estimator.

Keywords: geostatistic; robust estimator; spatial variability; wave model; weighted kappa.
Abbreviations: OLS: ordinary least squares; SDM: spatial dependence measure.

Introduction

Precision agriculture comprises the combination of contemporary agricultural practices, which aim to help the agricultural community improve production yield, use agricultural resources optimally, and minimize environmental impacts. Spatial interpolation prevails among the various resources; it uses a procedure that estimates the values of attributes in unsampled locations based on known locations values (Burrough et al., 2015).

There are several methods of spatial interpolation (Almasi et al., 2014; Malvić et al., 2020; Zeybek and Şanholu, 2020), which includes ordinary kriging, a popular geostatistical algorithm for interpolation and spatial estimation (Bai and Tahmasebi, 2021). Ordinary kriging is considered the best linear unbiased estimator of minimum variance (Isaaks and Srivastava, 1989).

To prepare maps using the ordinary kriging interpolator, it is necessary to model the spatial dependence structure of the studied phenomenon using estimators of the semivariance function. Several estimators of the semivariance function are available, with Matheron's classic estimator being the most used (Cressie, 1993). This estimator is not robust in the face of adversities in the data, such as the presence of outliers (Genton, 1998) and a proposed alternative is to use the Genton semivariance function estimator.

Although there are comparative works related to the estimators (Lark, 2000; Ruffa et al., 2015; Barbosa et al., 2019), comparative works considering theoretical semivariograms with cyclical behavior, such as the Wave model (Olea, 2006), are nonexistent. Precision agriculture commonly uses exponential, spherical, and Gaussian models (Oliver, 2010) as well as models of the Mátern family (Schemmer et al., 2017; Dalposso et al., 2021). These models are well adjusted when semivariances increase with distance until they plateau, which is why they are called increasing monotonic (Carvalho et al., 2009). However, the semivariogram is not restricted to this monotonic form, where decreasing or cyclic segments are observed. These nonmonotonic structures are known as "hole effects" and may or may not plateau and have reduced wave amplitudes and can be isotropic or anisotropic (Pyrcz & Deutsch, 2003). Neglecting these nonmonotonic structures in the analysis may result in erroneous interpretations, as the model adopted may not reproduce the observed variability patterns. Therefore, this study aims to compare the Matheron and Genton semivariance function estimators considering the Wave model adjustment for soybean yield data in the presence of an outlier.

Results and discussion

Exploratory analysis

The average soybean yield in the monitored area was 2.276 t ha^{-1}, below the 3.535 t ha^{-1} state average, and the 3.527 t ha^{-1} national average during the agricultural year 2020-2021 (Conab, 2021). Of the 101 sampling points collected, approximately 75 points presented soybean yield equal to or lower than 2.670 t ha^{-1} (third quartile) and the maximum observed value of 3.990 t ha^{-1} differed considerably from the other values, being characterized as an outlier (Figure 2). To investigate the existence of high or low sample values clusters, we elaborated the pos-plot graph presented in Figure 3.

Figure 3 shows that, generally, the highest soybean yield values (t ha^{-1}) are allocated in the region starting from the center of the monitored area and extends to the northern region. The remaining area, extending from the south to the central region, presents a greater number of samples classified in the first two classes of the graph, which characterizes it as a lower productivity region. The maximum value found is located in the eastern region of the monitored area.

Variogram analysis

Figure 4 presents the experimental semivariograms prepared with the Matheron and Genton semivariance function estimators, considering a complete set of all 101 sample points and also considering the outlier removal.

Although the experimental semivariograms functioned similarly, the outlier removal changed the estimated semivariances (Figure 4). This fact is more evident for estimates obtained through the Matheron semivariance function estimator, because, generally, the differences in absolute value between the semivariances estimated with the outlier and without the outlier are greater when compared to the same differences considering Genton semivariance function estimator.

In both the experimental semivariograms, the behavior of the first three semivariances increases and then decreases, finally followed by a rise in semivariances values thereafter (Figure 4). This behavior had already been observed in some studies related to precision agriculture (Santra et al., 2008; Amirinejad et al., 2011), and the best adjustments were obtained with the Wave model. This model is widely used when there is some periodicity in the data, resulting in a "hole effect" due to positive and negative correlations between different distant regions (Mahdi et al., 2020).

In view of this finding, the ordinary least squares (OLS) method was used to estimate the parameters of the spatial dependence structures observed in Figure 4. This was achieved using the Wave model, whose results are presented in Table 1. Considering the adjustments made with the complete set of data, it is observed that the models presented similar estimates for the nugget effect and the range parameter, where both indicated a moderate spatial dependence (Table 1).

When considering the adjustments made without the outlier, it is observed that the models presented a different behavior. While the model adjusted to the experimental semivariogram obtained with the Genton semivariance function estimator presented a behavior similar to the adjustments made with the complete set of data, the model obtained through the Matheron semivariance function estimator showed no nugget effect, and its range was considerably lower than the others, thereby indicating a weak spatial dependence (Table 1).

Thus, it is noteworthy that the outlier removal had an impact on the modeling performed considering the spatial structure estimated by Matheron's semivariance function.

Geostatistical mapping

Generally, as the interest of the analysis is not limited to modeling the structure of spatial variability and, in this case, it is desired to obtain a detailing of soybean yield (t ha^{-1}) that goes beyond what is allowed by the sampling points, we used the model's information to make the maps, as shown in Figure 5.

It is observed that the soybean yield behavior (t ha^{-1}) in maps prepared with all sampling points (Figures 5(a) and 5(b)) is similar, thereby highlighting the *outlier* region in the legend's last class. With the *outlier* removal, its region values no longer rank last in the legend in the map from the Genton semivariance function estimator (Figure 5(c)); however, other regions are not significantly impacted.

However, when comparing the soybean yield map (t ha^{-1}) obtained by adjusting the data without an outlier using the Matheron semivariance function estimator (Figure 5(d)), a considerable difference is noticeable. What is evidenced in this map are the various circular regions around the sampling points. This behavior had already been observed by Dalposso et al. (2018) in a map of soybean yield (t ha^{-1}). According to the authors, it is caused by the fact that the model's range is close to the minimum distance between sampling points. In this model's case, which has a range of 84.6 m (Table 1), and by observing the distance between all pairs of points used (Figure 1), it becomes evident that only 24 (0.47%) of the 5,050 possible pairs have a distance lower than or equal to the range. Thus, the vast majority of the pairs of points are at a greater distance than the spatial dependence radius indicated by the model, which justifies the appearance of circular regions, a phenomenon also known as the "bulls eye effect" (Menezes et al., 2016).

The outliers removal from the analysis is still controversial. Li and Heap (2008) defend it, arguing that it resulted in a considerable performance improvement of spatial interpolation methods. Schabenberger and Gotway (2004), on the contrary, argue that unless a measurement has been poorly sampled, the removal of extreme observations is condemnable because it reduces the number of pairs available for the semivariogram's preparation. Uribe-Opazo et al. (2012, 2021) also conducted studies on outliers removal and influential points, investigating how this withdrawal influences model choice, model parameters estimation, and the elaboration of thematic maps with different probability distributions.

Comparison of thematic maps

The Kappa ($\widehat{\mathrm{K}}$) and weighted Kappa ($\widehat{\mathrm{K}}_{\mathrm{w}}$) indices are used for studying comparing maps in a nonsubjective way, thereby quantifying the differences observed visually in maps. Table 2 presents the results obtained. General, the similarity between maps that considered the Matheron semivariance function estimator with and without outlier is weak ($\widehat{\mathrm{K}}$ and $\widehat{\mathrm{K}}_{\mathrm{w}} < 0.4$). When comparing the maps that considered the Genton semivariance function estimator with and without the outlier, it is verified that there is a high similarity between them ($\widehat{K}$ and $\widehat{K}_w \geq 0.75$).

Materials and methods

Study area and data

The soybean yield data (t ha^{-1}) used in this study was garnered during the agricultural year 2020-2021 in a commercial area of 167.35 ha located in the western region of Paraná, Brazil, close to the municipality of Cascavel, with

Table 1. Parameters estimated through ordinary least squares - OLS, considering the Wave model adjusted to experimental semivariograms of soybean yield (t ha^{-1}) and SDM index.

Data	Estimator	$\hat{\varphi}_1$	$\hat{\varphi}_2$	$\hat{\varphi}_3$	$\hat{a}$ (km)	SDM
Complete	Genton	0.0954	0.1319	0.0542	0.4853	26.67
	Matheron	0.0942	0.1607	0.0500	0.4481	25.67
Without outlier	Genton	0.1027	0.1025	0.0523	0.4686	23.89
	Matheron	0.0000	0.2148	0.0283	0.0846	06.10

$\hat{\varphi}_1$: Estimated nugget effect; $\hat{\varphi}_2$: Estimated contribution; $\hat{\varphi}_3$: Estimated range parameter; $\hat{a}$:Estimated range; SDM: Spatial dependence measure.

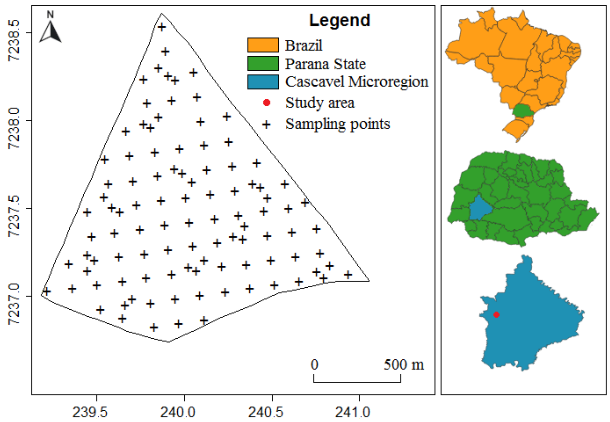

Fig 1. Location of 101 soybean yield sampling points (t ha $^{-1}$).

Table 2. Comparison between the maps obtained considering the estimators of the semivariance function of Genton and Matheron with and without outlier.

Comparison	$\hat{K}$	$\hat{K}_w$
Genton: complete set x Genton: wihout outlier	0.8138	0.8382
Matheron: Complete Set x Matheron: without outlier	0.2111	0.3185

$\hat{K}$: Kappa index; $\hat{K}_w$: weighted Kappa index.

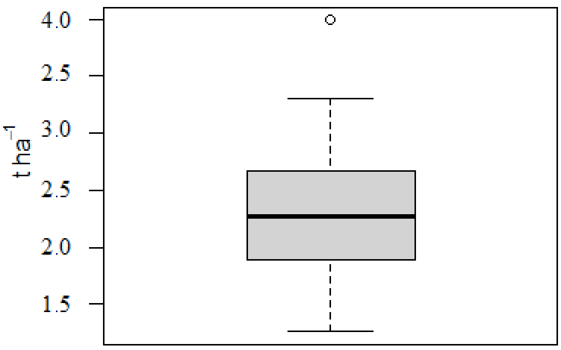

Fig 2. Soybean yield boxplot (t ha^{-1}) indicating the existence of an *outlier*.

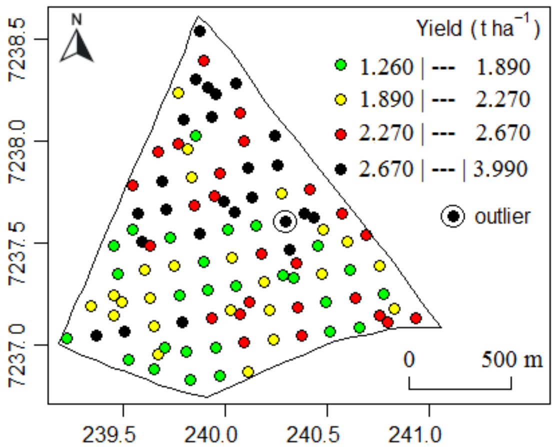

Fig 3. Soybean yield (t ha^{-1}) post-plot indicating the spatial distribution of the data separated by quartiles and the outlier location.

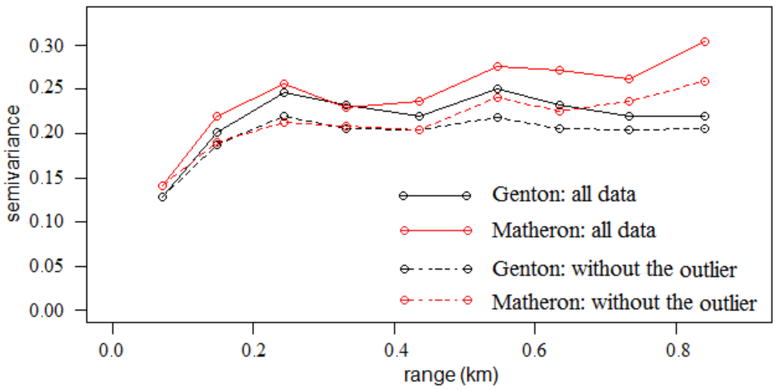

Fig 4. Omnidirectional experimental semivariograms of soybean yield (t ha^{-1}) prepared with the Matheron and Genton semivariance function estimators, considering a complete set of all 101 sample points and also considering the outlier removal.

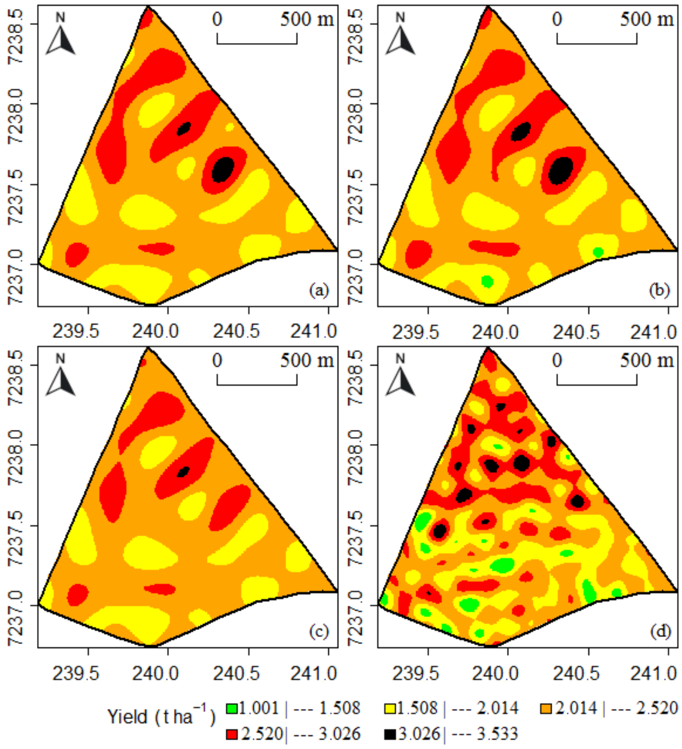

Fig 5. Soybean yield maps (t ha^{-1}) (a) using the Genton semivariance function estimator with all points, (b) using the Matheron semivariance function estimator with all points, (c) using the Genton semivariance function estimator without the outlier, and (d) using the Matheron semivariance function without the outlier.

the following coordinates: latitude of 24°57′18″S, longitude of 53°34′29″W, and average altitude of 714 m (Figure 1).
The regional climate is mesothermic and superhumid temperate and climatic-type Cfa (Köppen) as well as its soil is classified as dystroferric Red Latosol (Embrapa, 2013). The 101 sampling points were defined using a systematic sampling centered with pairs of close points (lattice plus close pairs) (Chipeta, et al., 2017) and were collected and tracked manually. After collection and screening, the samples were weighed and transformed into t ha^{-1}.

Geostatistical analysis

To model the spatial dependence structure of a regionalized variable, a stochastic process $\mathbf{Z} = \{Z(\mathbf{s}), \mathbf{s} \in S\}$ was considered, in which $s = (x, y)^T$ is the vector that represents a certain location in the studied area $S \subset \Re^2$, where $\Re^2$ is the two-dimensional Euclidean space. Suppose that the data $Z = (Z(s_1), \dots, Z(\mathbf{s}_n))^T$ of this second-order stationary process are isotropic, recorded in known locations $(\mathbf{s}_1, \dots, \mathbf{s}_n)$, and generated by the model $\mathbf{Z} = \mu\mathbf{1} + \boldsymbol{\varepsilon}$, where μ represents an unknown parameter to be estimated. $\mathbf{1}$ represents a vector of $n \times 1$ and $\boldsymbol{\varepsilon} = (\varepsilon(\mathbf{s}_1), \dots, \varepsilon(\mathbf{s}_n))^T$ represents a vector of random errors $n \times 1$, with normal n-variate distribution, with $E(\boldsymbol{\varepsilon}) = \mathbf{0}$ and covariance matrix, $\boldsymbol{\Sigma}$, $n \times n$, $\boldsymbol{\Sigma} = \boldsymbol{\Sigma}[(\sigma_{ij})] = C(Z(\mathbf{s}_i), Z(\mathbf{s}_j)), i, j = 1, \dots, n$.
In the parametric form (Uribe-Opazo et al., 2012; De Bastiani et al., 2015) the covariance matrix $\boldsymbol{\Sigma}$ can be defined as $\boldsymbol{\Sigma} = \varphi_1\mathbf{I}_n + \varphi_2\mathbf{R}(\varphi_3)$, in which $\mathbf{I}_n$ is the identity matrix, $\varphi_1 \geq 0$ is the parameter called nugget effect, $\varphi_2 \geq 0$ is the contribution parameter, $\varphi_3 \geq 0$ is the parameter that defines the range $(a = g(\varphi_3))$ of the model, and $R(\varphi_3) = [(r_{ij})]$ is a defined positive symmetric matrix. The elements r_{ij}, $i, j = 1, \dots, n$, represent the association between points $\mathbf{s}_i$ and $\mathbf{s}_j$, where $r_{ij} = 1$ if $i = j$ and $h_{ij} = 0$; $r_{ij} = 0$ if $i \neq j$

and $\varphi_2 = 0$; and $r_{ij} = \varphi_2^{-1}C(h_{ij})$ if $i \neq j$ and $\varphi_2^{-1} \neq 0$, where $C(h_{ij}) = C\left(Z(\mathbf{s}_i), Z(\mathbf{s}_j)\right)$ is the theoretical covariance function and $h_{ij} = \|\mathbf{s}_i - \mathbf{s}_j\|$ is the Euclidian distance between $\mathbf{s}_i$ and $\mathbf{s}_j$.

To identify the spatial dependence structure of soybean yield for stationary and isotropic stochastic processes, omnidirectional experimental semivariograms were constructed using Matheron (Cressie, 1993) (Equation (1)) and Genton (Genton, 1998) (Equation (2)) semivariance function estimators.

$$2\hat{\gamma}(h) = \frac{1}{N(n)} \sum_{i=1}^{N(h)} (Z(\boldsymbol{s_i} + \boldsymbol{h}) - Z(\boldsymbol{s_i}))^2, \quad (1)$$

where,
$\hat{\gamma}(h)$ is the estimator of Matheron semivariance function;
$Z(\mathbf{s}_i)$ is the value of variable Z at point $\mathbf{s}_i$,
$Z(\mathbf{s}_i + h)$ is the value of variable Z at point $\mathbf{s}_i + h$;
$N(h)$ is the number of pairs separated by distance h.

$$2\hat{\gamma}(h) = \left(Q_{N(h)}\right)^2, \quad (2)$$

where,
$\hat{\gamma}(h)$ is the estimator of Genton semivariance function;
$Q_{N(h)} = 2.2191\{|V_i(h) - V_j(h)|; i < j\}_{(k)}$;
$V_i(h) = Z(\mathbf{s}_i + h) - Z(\mathbf{s}_i)$;
2.2191 is the normal distribution consistency constant;
$k = \left(\frac{\left[\frac{N(h)}{2}\right]+1}{2}\right)$;
$\left[\frac{N(h)}{2}\right]$ denotes the whole part of $\frac{N(h)}{2}$.

The Wave model (Olea, 2006) presented in Equation (3) was used to model the spatial dependence structures obtained; the OLS method was used to estimate parameters.

$$\gamma(h) = \begin{cases} \varphi_1 + \varphi_2\left(1 - \frac{\varphi_3}{h}\operatorname{sen}\left(\frac{h}{\varphi_3}\right)\right), & h > 0 \\ 0, & h = 0 \end{cases} \quad (3)$$

After obtaining the adjusted models, the ordinary kriging interpolator was used to elaborate the thematic maps to estimate soybean yield values (t ha^{-1}) in unsampled locations.

Comparisons

The measurement of the spatial dependence degree of the adjusted models was obtained using the spatial dependence measure (SDM) of the Wave model developed by Neto et al. (2020), as shown in Equation (4).

$$SDM_{wave} = 0{,}637\left(\frac{\varphi_2}{\varphi_1+\varphi_2}\right)^{\frac{1}{2}} min\left\{1; \left(\frac{a}{0{,}5MD}\right)\right\} 100, \quad (4)$$

where,
a is the range;
MD is the maximum distance between two sampling points.

The SDM_{wave} is classified as weak dependence, if $0 \leq SDM \leq 21$, moderate dependence, if $21 < SDM \leq 34$, and strong dependence, if $34 < SDM \leq 63.7$ (Neto et al., 2020).

The similarity of interpolated maps is generally evaluated using the Kappa index ($\widehat{K}$) (Cohen, 1960). This work also considers the weighted Kappa index ($\widehat{K}_w$) (Cohen, 1968), presented in Equation (5), which uses weights (w_{ij}) to quantify unconformity.

$$\widehat{K}_w = \frac{\sum_{i=1}^{r}\sum_{j=1}^{r} w_{ij}P_{ij} - \sum_{i=1}^{r}\sum_{j=1}^{r} w_{ij}P_{i+}P_{+j}}{1 - \sum_{i=1}^{r}\sum_{j=1}^{r} w_{ij}P_{i+}P_{+j}}, \quad (5)$$

where,
$w_{ij} = 1 - |i - j|/(r - 1)$ are the linear weights (Cicchetti & Allison, 1971) for a contingency matrix with r classes, for $i, j = 1, \ldots, r$;
P_{ij} are the joint proportions i.e., the pixel count in each contingency matrix cell divided by N, the total number of pixels in the map, for $i, j = 1, \ldots, r$;
$P_{i+} = n_{i+}/N$ are the marginal proportions, where n_{i+} represents the sum of the pixels of the contingency matrix line i, $i = 1, \ldots, r$;
$P_{+j} = n_{+j}/N$ are the marginal proportions, where n_{+j} represents the sum of the pixels in the contingency matrix column j, $j = 1, \ldots, r$.

The interpretation of the magnitude of the weighted Kappa index is equivalent to that of the Kappa index (Fleiss et al., 2003), which $\widehat{K}_w \geq 0.75$ indicates a high similarity, $0.4 < \widehat{K}_w < 0.75$ indicates moderate similarity, and $\widehat{K}_w \leq 0.4$ indicates low or insufficient similarity.

Computational Resources

All analyses were performed using the R software (R Core Team, 2021). The experimental semivariances were calculated using the georob package (Papritz, 2016). Functions from the geoR package were used to adjust the models and elaborate the thematic maps (Ribeiro Jr. & Diggle, 2001). The vcd package was used to calculate the weighted Kappa and Kappa indices (Meyer et al, 2021).

Conclusion

The outlier removal altered the estimated semivariances, a less striking fact when the Genton semivariance function estimator was used. In relation to the Wave model, it was adequate to characterize the spatial dependence structure of soybean yield, and the evidenced behavior was the sensitivity of the Matheron semivariance function estimator to outlier presence, providing models with distinct characteristics. The differences between the models adjusted using the Matheron estimator with and without the outlier were distinctive in the thematic maps of soybean yield. After the outlier removal, the map started to present a considerable number of circular regions, which would make localized inputs application difficult. The weighted Kappa index proved to be a promising alternative for comparing maps, considering that it considers the different levels of disagreement between categories. Based on this comparative analysis, it was observed that the outlier exclusion provided fewer changes in the geostatistical modeling by considering the Genton semivariance function estimator, thus confirming its robustness.

Acknowledgments

Council for Scientific and Technological Development (CNPq); Coordination for the Improvement of Higher

Education Personnel (CAPES); Post-Graduate Program in Agricultural Engineering of Western State University of Paraná (PGEAGRI-UNIOESTE); Federal Technological University of Paraná (UTFPR) and Spatial Statistics Laboratory (LEE-UNIOESTE).

References

Almasi A, Jalalian A, Toomanian N (2014) Using OK and IDW methods for prediction the spatial variability of a horizon depth and OM in soils of Shahrekord. Environ Earth Sci. 4(15): 17-27.

Amirinejad AA, Kamble K, Aggarwal P, Chakraborty D, Pradhan S, Mittal RB (2011) Assessment and mapping of spatial variation of soil physical health in a farm. Geoderma. 160: 292-303.

Bai T, Tahmasebi P (2021) Accelerating geostatistical modeling using geostatistics-informed machine learning. Comput Geosci. 146: 104663.

Barbosa DP, Bottega EL, Valente DSM, Santos NT, Guimarães WD (2019) Delineation of homogeneous zones based on geostatistical models robust to outliers. Rev Caatinga. 32(2): 472 – 481.

Burrough PA, McDonnell RA, Lloyd CD (2015) Principles of geographical information systems 3rd edn. Oxford: Oxford University Press. 320 p.

Carvalho JRP de, Vieira SR, Greco CR (2009) Comparação de métodos para ajuste de modelos de semivariograma da precipitação pluvial anual. Rev Bras de Eng Agricola e Ambient. 13(4): 443-448.

Chipeta MG, Terlouw DJ, Phiri KS, Diggle PJ (2017) Inhibitory geostatistical designs for spatial prediction taking account of uncertain covariance structure. Environmetrics. 28(1): e2425.

Cicchetti DV, Allison T (1971) A new procedure for assessing reliability of scoring EEG sleep recordings. Am J EEG Technol. 11(3): 101–110.

Cohen J (1960) A coefficient of agreement for nominal scales. Educ Psychol Meas. 20(1): 37-46.

Cohen J (1968) Weighted kappa: nominal scale agreement with provision for scale disagreement or partial credit. Psychol. Bull. 70(4): 213-220.

Conab (2021) Séries históricas: soja Brasil – série histórica de produtividade – safras 1976/1977 a 2020/2021. < https://www.conab.gov.br/info-agro/safras/serie-historica-das-safras?start=30>

Cressie N (1993) Statistics for spatial data. New York : John Wiley & Sons. 928 p.

Dalposso GH, Uribe-Opazo MA, Johann JA, Galea M, De Bastiani F (2018) Gaussian spatial linear model of soybean yield using bootstrap methods. Eng Agrícola. 38(1): 110-116.

Dalposso GH, Uribe-Opazo, MA, De Bastiani, F (2021) Spatial-temporal Analysis of Soybean Productivity Using Geostatistical Method. J Agric Stud. 9(2): 283-303.

De Bastiani F, Cysneiros AHMA, Uribe-Opazo MA, Galea M (2015) Influence diagnostics in elliptical spatial linear models. Test. 24(2):322-340.

Embrapa (2013) Sistema Brasileiro de Classificação de Solos. 3rd edn. Brasília: Embrapa Solos. 353p.

Fleiss JL, Levin B, Myunghee C P (2003) Statistical Methods for Rates and Proportions. 3rd edn. Nova Jersey: John Wiley. 800 p.

Genton MG (1998) Highly Robust Variogram Estimation. Math Geol. 30(2): 213-221.

Isaaks EH, Srivastava RM (1989) An introduction to applied geostatistics. New York: Oxford University Press, 560 p.

Lark RM (2000) A comparison of some robust estimators of the variogram for use in soil survey. Eur J Soil Sci. 51(1): 137-157.

Li J, Heap AD (2008) A Review of Spatial Interpolation Methods for Environmental Scientists. Canberra: Geoscience Australia. 137 p.

Mahdi E, Abuzaid AH, Atta, AMA (2020) Empirical variogram for achieving the best valid variogram. Commun Stat Appl Methods. 27:547-568.

Malvić T, Ivšinović J, Velić J, Sremac J, Barudžija, U (2020) Application of the Modified Shepard's Method (MSM): A Case Study with the Interpolation of Neogene Reservoir Variables in Northern Croatia. Stats. 3(1): 68-83.

Menezes MD, Silva SHG, Mello CR, Owens PR, Curi N (2016) Spatial prediction of soil properties in two contrasting physiographic regions in Brazil. Sci Agric. 73(3): 274-285.

Meyer D, Zeileis A, Hornik K (2021) vcd: Visualizing Categorical Data. R package version 1.4-9. <https://CRAN.R-project.org/package=vcd>

Neto EA, Seidel EJ, Oliveira MS (2020) Geostatistical-based index for spatial variability in soil properties. Rev. Bras. Cienc. Solo. 44:e0200086.

Olea RA (2006) A six-step practical approach to semivariogram modeling. Stoch Environ Res Risk Assess. 20(5): 307-318.

Oliver MA (2010) Geostatistical Applications for Precision Agriculture. Dordrecht: Springer. 331 p.

Papritz A (2016) georob: Robust Geostatistical Analysis of Spatial Data. R package version 0.3-1. <https://CRAN.R-project.org/package=georob>

Pyrcz M Deutsch C (2003) The whole story on the hole effect. In: Searston S (ed) Geostatistical Association of Australasia Newsletter, 18, West Perth, Australia, 18 p.

Ribeiro Jr PJ, Diggle PJ (2001) geoR: A Package For Geostatistical Analysis. R News. 1(2): 15–18.

R Core Team (2021) R: A language and environment for statistical computing. R Foundation for Statistical Computing, Vienna, Austria. <https://www.R-project.org>

Ruffa S, Vicario G, Pistone, G (2015) Analysis of the Covariance Structure in Manufactured Parts. Commun Stat - Theory Methods. 44: 4540–4551.

Santra P, Chopra UK, Chakraborty D (2008) Spatial variability of soil properties and its application in predicting surface map of hydraulic parameters in an agricultural farm. Curr Sci. 95(7): 937-945.

Schemmer RC, Uribe-Opazo MA, Galea M, Assumpção RAB (2017) Spatial variability of soybean yield through a reparameterized t-student model. Eng Agrícola. 37(4): 760-770.

Uribe-Opazo MA, Borssoi, JA, Galea M (2012) Influence Diagnostics in Gaussian Spatial Linear Models. J Appl Stat. 39(3): 615-630.

Uribe-Opazo MA, De Bastiani F, Galea M, Schemmer RC, Assumpção RAB (2021) Influence diagnostics on a reparameterized t-Student spatial linear model. Spat Stat. 41:100481.

Schabenberger O, Gotway CA (2004) Statistical Methods for Spatial Data Analysis. Boca Raton: Chapman & Hall/CRC. 512 p.

Zeybek M, Şanhoğlu, Í (2020) Investigation of landslide detection using radial basis functions: a case study of the Tas¸kent landslide, Turkey. Environ Monit Assess. 192(4): 230.